

Remote sensing monitoring of vegetation area and species diversity over 15 years in Sirjan Salt Lake, Iran

Reza Atighi, Abbas Ahmadi*, Javad Varvani, Hamid Toranjzar, Nourollah Abdi

Department of Natural Resources, Islamic Azad University, Arak, Iran.

*Corresponding author: a-ahmadi@iau-arak.ac.ir

Received 11 January 2021; Accepted 11 March 2022; Published online 4 July 2023

Abstract:

This study was aimed to investigate the changes in surface and vegetation cover of the Sirjan Salt Playa (SSP) located in Kerman, Iran using Remote Sensing (RS) data. The ASTER data from 2002, 2008, and 2013 were used as the main tool. Also, using the Normalized Difference Vegetation Index (NDVI) on satellite data, the vegetation area and species diversity were determined. The research technique was correlation and comparison methods, and data analyses were made using SPSS and Edrisi software. Result showed that RS systems, in some ways, have a very good ability to study developments in desert areas. Based on the results of 15 years evaluation, the area of SSP was changed in different years and the vegetation area was changed in each period compared to the previous period, but vegetation diversity was not changed in this area. After extracting the vegetation map using NDVI index, considering the mean and standard deviation in satellite images of each period, the vegetation of the study area was divided into four classes of good, average, very poor and no vegetation. Also, the results showed that the area of good vegetation cover was 19278 ha in 2002, which increased to 22971 ha in 2008 and decreased by 20499 ha in 2013 compared to 2008. The medium vegetation class comprised 104985 ha of the land in 2002, which increased to 136128 and 108340 ha in 2008 and 2013, respectively. The kappa coefficient obtained from the comparison of the vegetation map using NDVI index and land cover map for 2002, 2008, and 2013 were 0.81, 0.83, and 0.84, respectively, which gave higher values than the SAVI vegetation index. Generally, the study suggested using other indices as NDVI and Soil-Adjusted Vegetation Index (SAVI) indices in arid lands and playa margins, with very poor vegetation cover.

Keywords: Remote sensing; Vegetation; Sirjan salt; NDVI index; ASTER

1. Introduction

The Sirjan salt marsh is referred to as one of the largest salt reservoirs in Iran which turns into a large and a wavy lake at times of rainfall in the Sirjan desert in a few hours and attracts thousands of tourists from different cities of Kerman and Fars provinces, Iran. While it is filled with water after rainfall due to flooding of the surrounding plains, this area being known as the salt marsh after the evaporation of water in this season witnesses a thick cover of table salt on the desert, which covers thousands of hectares. In general, there is not enough information available about saline lands and their potential in the country so that this information cannot be the basis of appropriate planning [1, 2]. The term “salt marsh” or “salinization of soils” is the accumulation of a certain amount of soluble salt on the surface

crust of the earth, i.e. the soil, where the surface soil crust loses its capability as the place of growth and development of plants due to the biological activity taking place in this part [3]. Different factors affect the accumulation of salts and salinization of soils, which are collectively divided into two intrinsic (genetic) and acquired factors [4]. The most important factors are geomorphological and hydrological conditions (entry of saline water into the region, the proximity of groundwater aquifers to the ground typically < 50 m), transfer of salts by wind and biological factors, and the impact of human activities [5]. Salinity and alkalinity resulting from the accumulation of salts and bases together with inadequate natural drainage are both associated with drought and inadequate drainage [3]. On the other hand, plants that grow and complete their life cycles in habitats

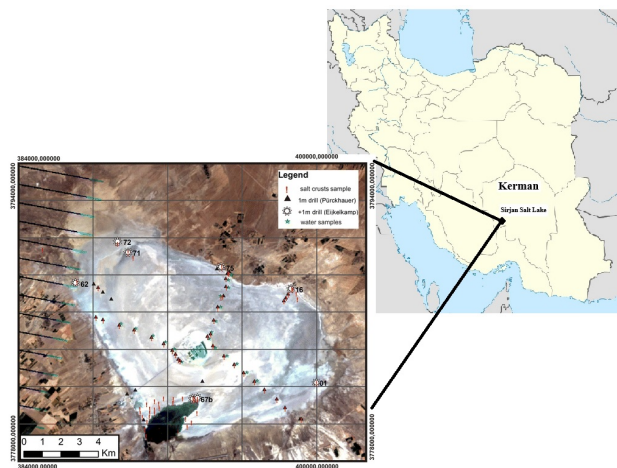


Figure 1. Geographical position of the Sirjan Salt lake in Iran's map.

with high salt concentrations are called halophytes, a term usually used only for plants found in permanent saline habitats [6, 7]. The actual range of plant distribution and the impact of certain environmental factors on plant zonation is not easily detectable in halophyte communities [8, 9]. As such, the zonation of halophytes includes stem succulent plants, leaf succulent plants, and halophytes depending on the distance from the center of salinity (reduction of salt levels) [10]. Very saline and saline soils have a large morphological and chemical diversity; therefore, due to the high physical, chemical, and biological complexities of soil, it is reasonable to expect soil spectral complexities. This has led to different spectral reflections from the salt marshes [3].

There are also studies conducted in this area. Nateghi et al. reported that 21% of mangrove forest area and 60% of agricultural lands and natural vegetation within Qeshm Island were added during 13 years [11]. Pour Khosravani et al. showed that the vegetative forms of plants were effective in explaining the formation and evolution of Nebkas [12]. The presence of different relationships between the morphometric components of Nebkas and vegetation indicates the different performance of species in the development of Nebkas. According to Yamani and Mazidi, NDVI is the best indicator for the study of vegetation in a study area [13]. Ahmadi Nodooshan et al. studied the changes in the land cover of Arak city using RS and GIS [14]. The results showed a significant increase in the area of the city, a decrease in vegetation and barren lands and the stability of the mountain class between 1985 and 2010. Yarahmadi investigated the role of Lake Urmia in atmospheric parameters of temperature, precipitation, and humidity using the "Technology and Atmospheric Mission Platform" (TAMP) model [15]. Kardan et al. evaluated the capability of the Air Pollution Modelling (TAMP) model (version 3) to simulate atmospheric parameters in the Jazmourian pit in Kerman province, Iran [16]. Zhou et al. showed that air temperature, wind speed and direction, and energy balance would change by the reduction and elimination of regional lakes [17]. Sun et al. implemented a monthly NDVI time-series from HJ-1 optical imagery to reflect salt marshes [18]. They achieved

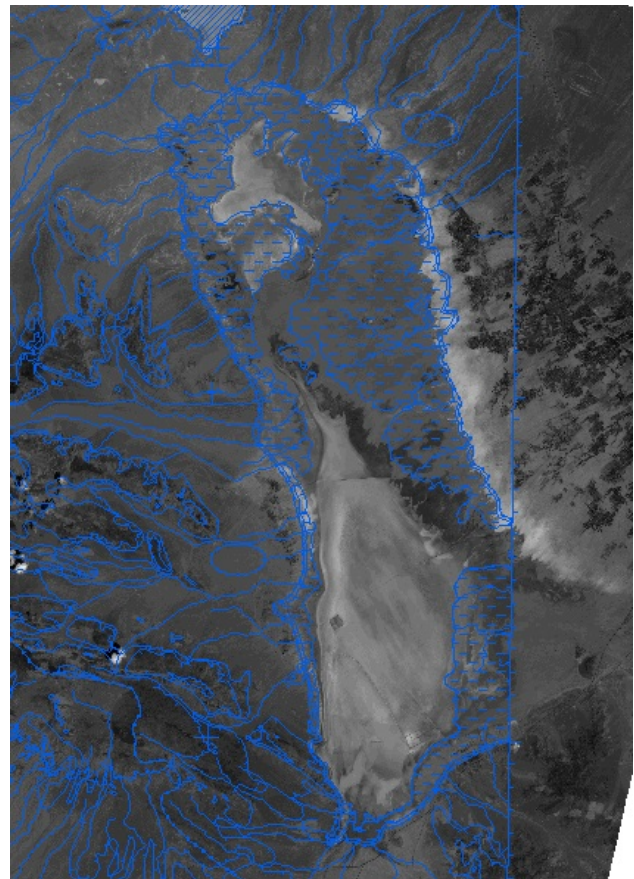


Figure 2. Chavez's Geometric corrections using a topographic-based map with an accuracy of 90%.

the overall accuracy of the salt marsh mapping equal to 90.3%. After 2 years, Sun et al. applied the monthly NDVI time-series to all viable Landsat TM/ETM + images [19]. They found that the upper low marsh vegetation community has diminished by 19.4% in the study period. Mardi et al. found that in the last two decades, the pollution caused by the suppression of emissions of salts on the Lake Urmia border, as the major regional aerosol source, has doubled [4]. Westinga et al. utilized hyper-temporal NDVI imagery to optimize the hierarchical vegetation mapping and achieved high accuracy results [20]. Maneja et al. implemented a ground-based survey and NDVI time-series to assess the resilience of offshore islands' ecosystems in the Saudi waters [21]. They found that any reduction in island vegetation may lead to island desertification.

Located in the southeast of Iran, Kerman province is one of the major arid and desert regions of the country. The study of these areas requires detailed fieldwork and seasonal constraints and natural barriers, particularly in desert areas, and other problems such as cost, time, and facilities and equipment provide many constraints. Therefore, the most appropriate method is to use RS and its efficient techniques [22]. Perhaps, one of the most important capabilities of this system is the pervasiveness, observation, and frequent study of desert phenomena to examine the evolutionary trends over successive and even short-term periods. In This research, it is tried to partially investigate changes

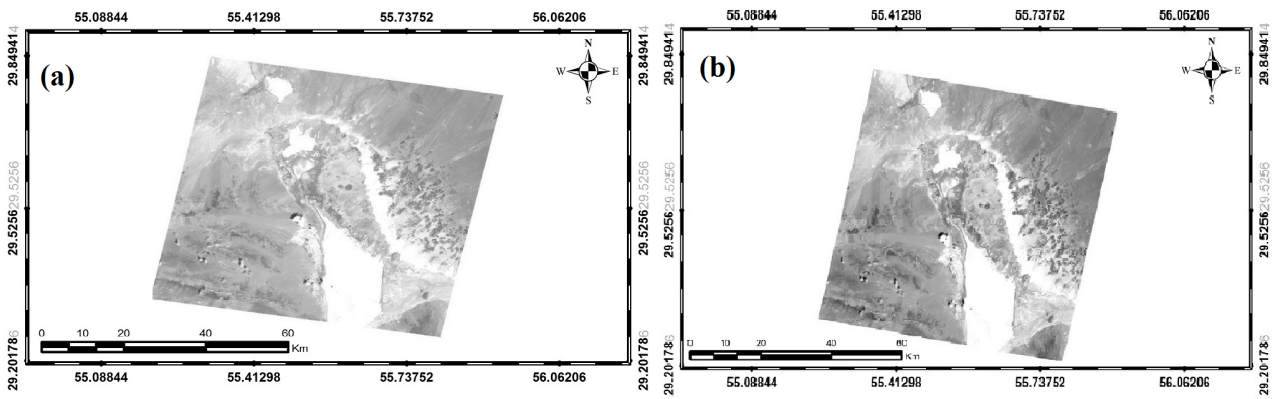


Figure 3. Atmospheric and reflection corrections of images from 2002; (a) before and (b) after correction.

in the Sirjan salt marsh, including changes in vegetation and salt marsh, with the help of RS data.

2. Materials and methods

Sirjan Salt Playa (SSP) catchment area, which is one of the sub-basins of the Gavkhooni swamp, was investigated in this study (Fig. 1). The area geographical coordinates are $56^{\circ} 26' 31''$ to $30^{\circ} 54' E$ and $35^{\circ} 30' 27'' N$, the region encompasses large parts of Sirjan and Shahrabak and a small part of Yaft city (Fig. 1). The area of this basin is 442779 ha and its minimum and maximum altitudes above sea level are 56 and 1754 m, respectively. Due to a high altitude difference (> 1698 m) between the highest and lowest altitude points, the area has relatively high climatic diversity. The annual precipitation varies from 120 to 350 mm with an average of about 180 mm. More than 65% of precipitation occur in winter. The highest rainfall occurred in the

cold months of the year (January, February and March), and the lowest rainfall occurred from June to October. The annual evaporation and the average annual temperature in the region are 2185 mm and $16.1^{\circ}C$, respectively. The study area is located between the central and the eastern Zagros Mountains and its most important heights are Panj, Chahar Gonbad, and Ain-al-Baqar mountains. The SSP is seen as a dent in the region. Magmatic activity in this area includes acidic intrusions in the Hajiabad-Sirjan areas, which are often in the forms of granite and diorite and are observed in the form of small and large batholiths. Granites and diorites are also related to the orogenic phase and Laramide Folding formed as batholiths, etc. In this region, the main source of rainfall is in the western air mass and the effect of humid air is in the Indian Ocean. The most important rivers of Sirjan are the Tangoyeh (Palangi) and Hossein Abad rivers, both of which are seasonal.

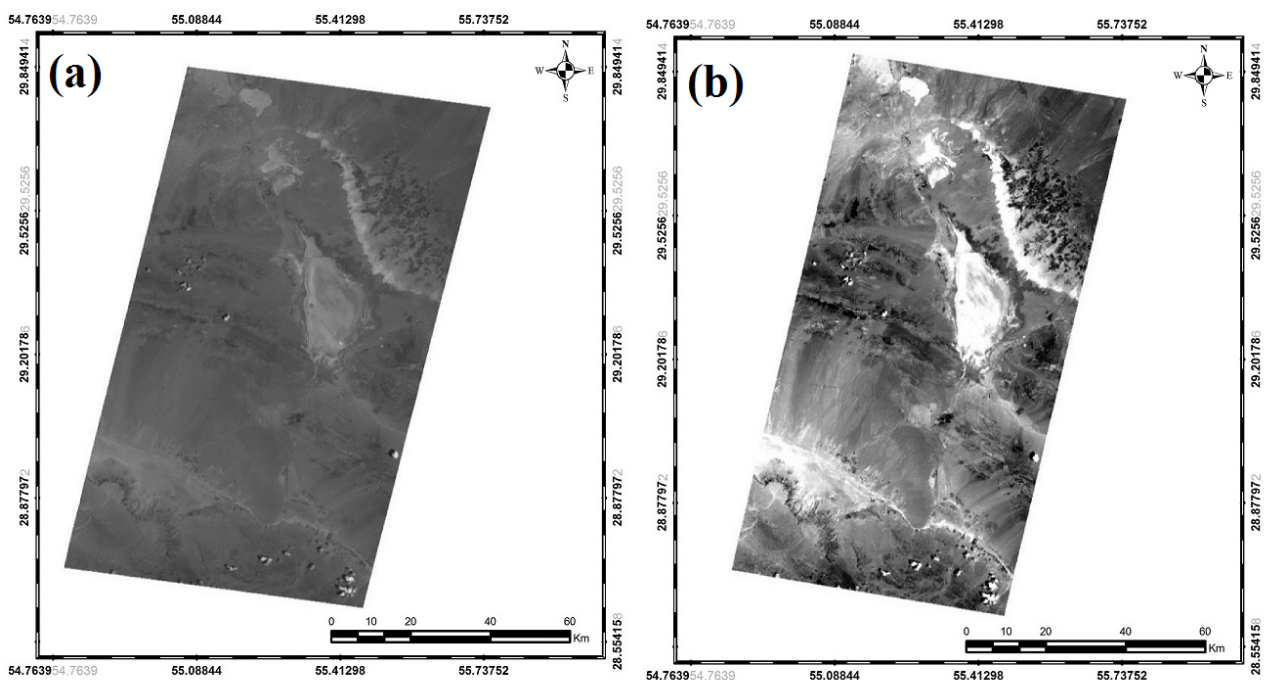


Figure 4. Atmospheric and reflection corrections of images from 2008; (a) before and (b) after correction.

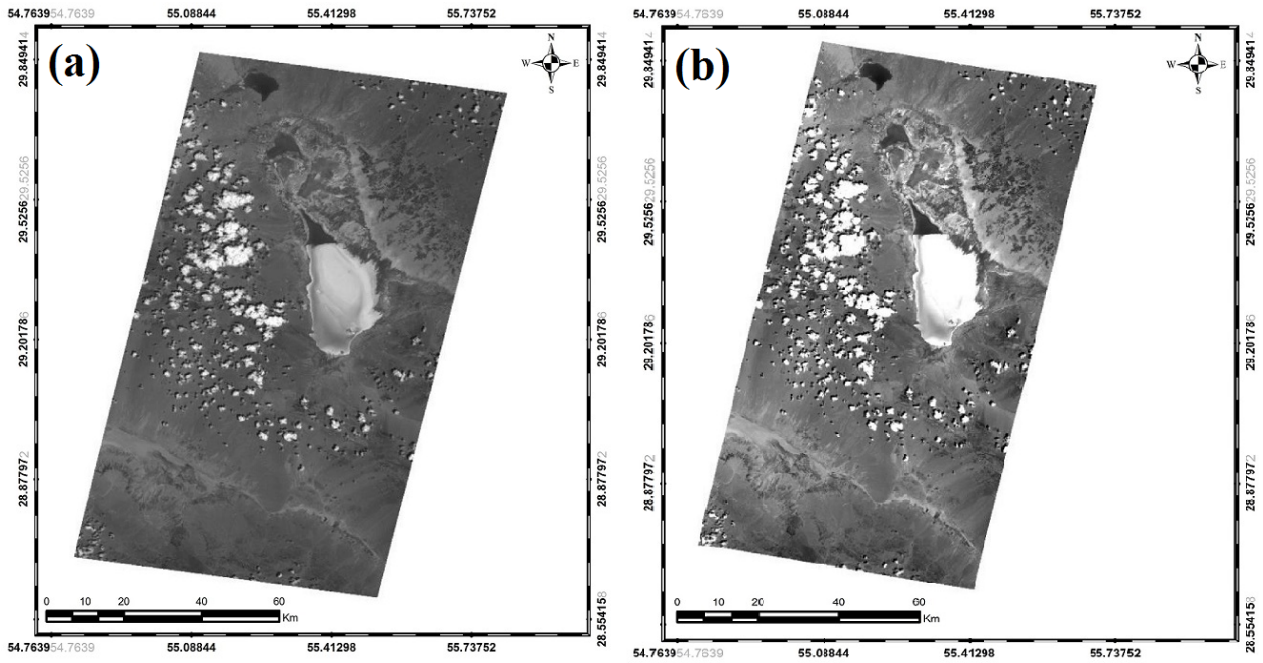


Figure 5. Atmospheric and reflection corrections of images from 2013; (a) before and (b) after correction.

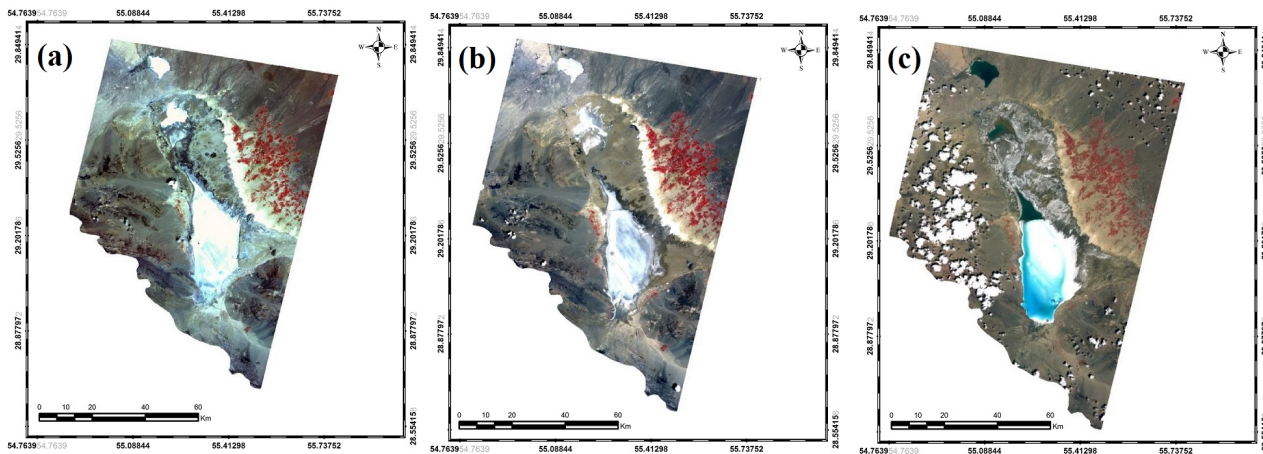


Figure 6. Combinations of different bands and making a false-color image; (a) 2002, (b) 2008, (c) 2013.

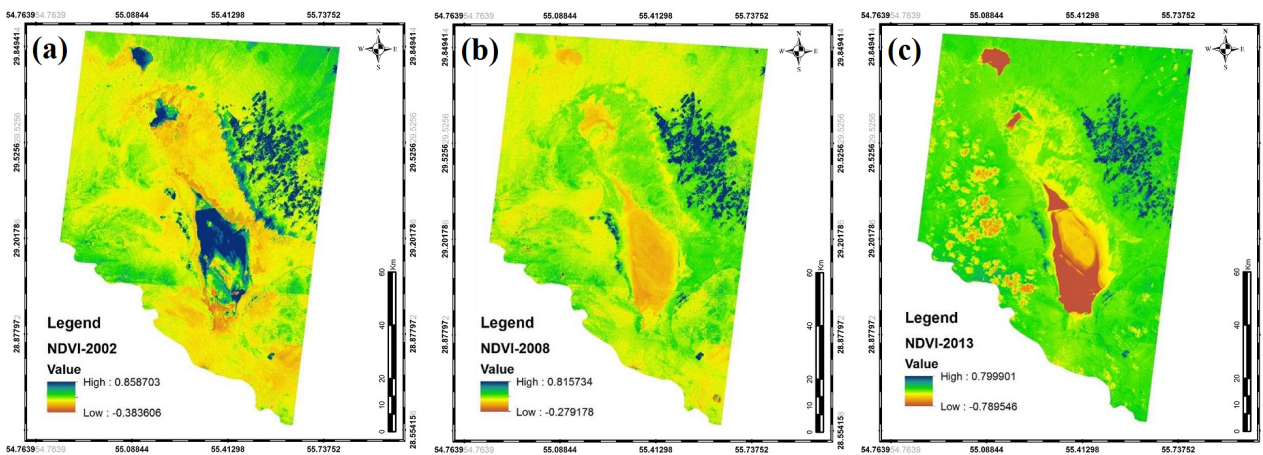


Figure 7. Classification of the vegetation index; (a) 2002, (b) 2008, (c) 2013.

Table 1. Results of PCA and percentage variance of information in the first three components.

T-Mode		PCA 1	PCA 2	PCA 3
T-Mode Component	T-Mode Eigenvalue	0.033	0.000	0.000
	% Var	99.278	0.634	0.087
		PCA 1	PCA 2	PCA 3
	B1-2008	0.994	-0.099	0.041
	B2-2008	0.998	-0.044	-0.035
	B3-2008	0.995	0.090	0.008

At weather station Sirjan, the average long-term annual rainfall and temperature are about 150 mm and 17 °C, respectively. The study area is called Keffeh Namak (salt marsh) in the Sirjan desert catchment area, which is located 35 km west of Sirjan city.

The information used for the present study is the ASTER satellite imagery. The vegetation products of ASTER sensor related to Terra satellite for 2002 (May 9), 2008 (May 26), and 2013 (May 7) were used here because one of the important goals of this research was to study and discover changes over some time. The spectral range in which images are obtained is three bands in the visible and near-infrared spectral range (VNIR subsystem), six bands in the short-wavelength infrared range (SWIR subsystem), and five bands in the thermal infrared range (TIR subsystem). The images received in three spectral ranges had different spatial resolutions. VNIR and SWIR bands had spatial resolutions of 15 and 30 m, respectively, while thermal infrared images had a spatial resolution of 90 m.

In this research, the type, amount, changes, and expansion of vegetation were determined using the normalized difference vegetation index (NDVI) on two series of satellite data from 2002, 2008, and 2013 using correlation and comparison methods. In this regard, the prepared satellite images were first subjected to processing. NDVI is very suitable for the representation of vegetation biomass, leaf area index, plant production, and vegetation segregation, which is calculated using Equation (1) [23]:

$$NDVI = \frac{NIR - RED}{NIR + RED} \tag{1}$$

Where NIR and RED are reflections in the near-infrared and the red bands, respectively. Theoretically, the value of this index ranges between +1 and -1. The bands 2 – 3 of the ASTER sensor, abbreviated as b1, b2, and b3, were used in this study. One of the necessary steps in RS studies is the extraction of digital information such as sampled ground points, which is time-consuming and requires a careful examination. For this purpose, the coordinates of the ground points specified by GPS must be determined on the image. For more convenience, a point peel was created from the coordinates of the points sampled in the field operation. The sampling method consists of three pixels, i.e. each sample represents three pixels. Therefore, it seemed necessary to calculate and determine the average spectral value of three pixels as a sampling point to obtain different statistical analyses between soil samples with different factors and the spectral values of the sample points. The software used in this section was Idrisi. Also, according to the error matrix Tables (Tables 3, and 4), the indicators of the product accuracy, user accuracy, and kappa coefficient, the calculation, and accuracy of the final map were tested. The result obtained from the error matrix was considered from the user accuracy, producer accuracy, and overall accuracy of the classification result.

3. Results

3.1 Preprocessing of images

Satellite images should be examined for streaks, misalignment of scan line clusters, duplicate pixels, and atmospheric errors such as cloud spots. To this end, different bands of the ASTER sensor were reviewed separately after im-

Table 2. Characteristics of vegetation classes and NDVI value for the periods of 2002, 2008, and 2013.

Classes Period	NDVI Value		
	2002	2008	2013
Good vegetation	0.1 – 0.86	0.096 – 0.816	0.15 – 0.78
Medium vegetation	0.039 – 0.1	0.044 – 0.096	0.042 – 0.15
Very poor vegetation	-0.022 – 0.039	-0.008 – 0.044	-0.073 – 0.042
No vegetation	-0.383 – -0.022	-0.279 – -0.008	-0.789 – -0.073

Table 3. Kappa coefficient values and overall accuracy of plant indices.

Plant indices	2002		2008		2013	
	Kappa coefficient	Overall accuracy (%)	Kappa coefficient	Overall accuracy (%)	Kappa coefficient	Overall accuracy (%)
NDVI	0.81	85	0.83	87	0.84	89
SAVI	0.75	81	0.79	82	0.81	86

proving the contrast and also as color combinations with different magnifications, and different correction operations were performed on individual images.

Geometric correction operations of the ASTER sensor bands related to May 7, 2002, June 25, 2008, and May 7, 2013 were performed in Idrisi software using 15 ground control points with an RMSE error of 0.46 pixels. The accuracy of the geometric corrections was examined with the topographic map of the study area using the vector layer of roads and the routes taken via GPS. By overlaying this layer on the matching images, the geometric correction of the images was confirmed more accurately. Fig. 2 depicts a corrected sample image. The purpose of geometric correction is to compensate for deviations. Topographic maps of 1: 50,000 of the Army Geographical Organization were used to geometrically match the images. The images were geometrically matched using a half-pixel geometric error (RMS = 0.5) using ground control points. In the next step, for geometric correction of the images, geo-coding was done using the image sampling method so that all the images are geometrically compatible with each other and obtain the same conditions. The images were geometrically matched using a half-pixel geometric error (RMS = 0.5) using ground control points. In this research, Chavez's method was used for atmospheric correction [24]. Figs.

(3), (4), and (5) show atmospheric reflectance corrections for images from 2002, 2008, and 2013. It shows the high performance of atmospheric and reflection corrections of images from 2002, 2008, and 2013 before the correction processes in each stage.

3.2 Modeling vegetation surface and main bands

In this study, only near-infrared (b3) and red (b2) bands with correlation coefficients of 92% and 95%, respectively had significant relationships with vegetation characteristic ($P < 0.01$). Since the absorption and transmission of electromagnetic energy are very low and the reflection rate is high in the near-infrared range (Safdar et al.), the significant relationship between the vegetation surface and the near-infrared band can be attributed to a high reflection of vegetation in this area [25]. Also, the sparse vegetation in most arid areas has created special conditions in terms of the reflection type and causes the substrate soil to affect and dominate the plant reflection effect.

Examination of tables obtained from the principal component analysis (PCA) determined the participation percentage of each band in the construction of different components and the variance percentage of each component. Table (1) represents the information about the components obtained from bands 1, 2, and 3 of the ASTER sensor. The first

Table 4. Accuracy of classifying images in years of 2002, 2008, and 2013.

Index	Classes of vegetation condition	2002		2008		2013	
		User accuracy	Product accuracy	User accuracy	Product accuracy	User accuracy	Product accuracy
NDVI	Good	89.27	75.63	84.72	94.17	88.14	92.87
	Medium	98.18	99.47	98.27	97.35	99.11	97.36
	Very poor	97.55	92.38	89.81	88.13	84.25	88.14
	No vegetation	53.19	76.18	87.45	81.47	69.51	77.43
SAVI	Good	91.43	84.77	75.24	76.44	81.29	82.55
	Medium	98.28	97.72	98.33	97.64	95.87	94.88
	Very poor	96.55	84.66	94.23	95.56	79.46	86.39
	No vegetation	67.48	77.47	63.22	66.38	77.11	84.91

Table 5. Vegetation classes and the area of each class.

Vegetation class	Area in each period (ha)		
	2002	2008	2013
Good	19278	22971	20499
Medium	104985	136128	108340
Very poor	283786	253346	284308
No vegetation	34730	30334	29632
Sum	442779	442779	442779

component obtained from the PCA has the highest percentage variance of information, which indicates the level of information transferred to this component so that the first components account for 99% of the information (Table 1). In the subsequent components, the amount of information is lower than that in the first comparison. In this study, therefore, the first component of the three transformations was added as artificial bands to the existing bands for digital analysis.

After the calculation of the utility index, the combination of bands 1, 2, and 3 was selected among a combination of different bands according to the resolution of composite images and possible detection of topologies. Fig. 6 displays the combination of the main bands for creating a false-color image.

3.3 Results of image classification

After the necessary processing on satellite information in terms of geometric and atmospheric corrections, it

is necessary to convert the data into a usable form for vegetation assessment, for which Vegetation Indices (VIs) were used based on combining the bands for the evaluation of the relationship between plant indices and reflections. NDVI is one of the most widely used indices for monitoring vegetation changes. NDVI values range from -1 to 1, with higher values indicating denser vegetation. It was implemented to reclassify NDVI maps as referring to vegetation rates based on spectral reflections (Bharathkumar and Mohammed-Aslam) [26].

To investigate the qualitative changes in vegetation during 15 years, NDVI output maps were classified into four vegetation classes (good, medium, very poor, and no vegetation) based on means and standard deviations [27].

Class 1): Values smaller than the average minus the standard deviation

Class 2): Mean minus standard deviation to average

Class 3): Mean to mean plus standard deviation

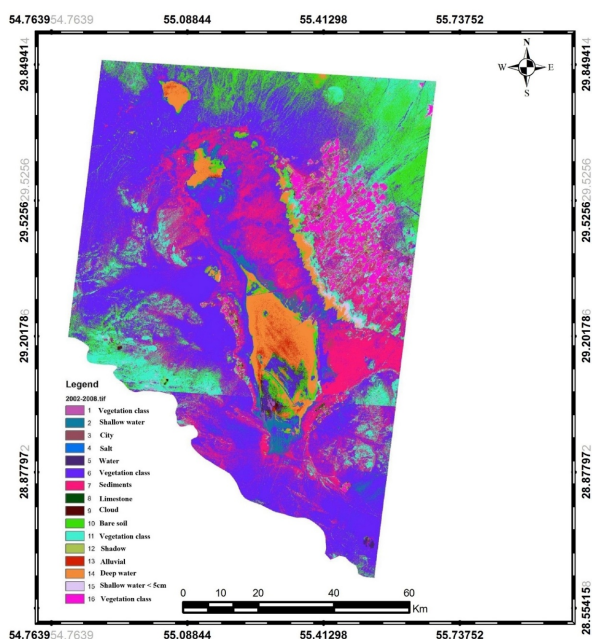


Figure 8. The rate of vegetation change in 2008 compared to 2002.

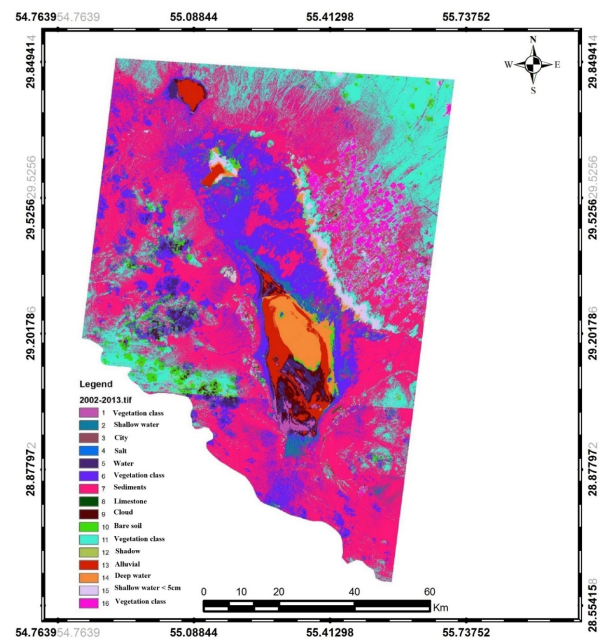


Figure 9. The rate of vegetation change in 2013 compared to 2002.

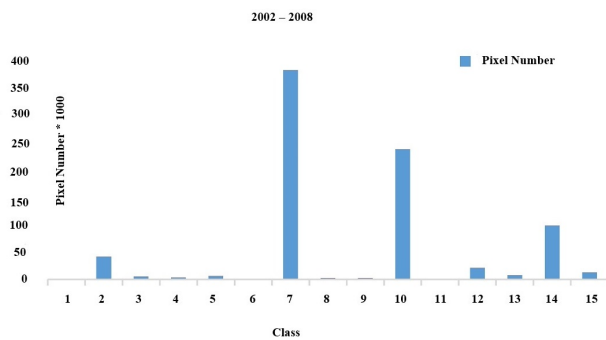


Figure 10. The amount of vegetation changes from 2002 to 2008 in each of the codes.

Class 4): Values greater than the mean plus the standard deviation

Table (2) lists the values of each class for the periods of 2002, 2008, and 2013. Based on Table (2), the vegetation index in the four classes was prepared for each period. Also, Fig. 7 presents the classification of the vegetation index. It indicates that the area of good vegetation cover was increased in 2008 and decreased in 2013. The medium vegetation class increased in 2008 and decreased in 2013. The very poor class decreased 2008 and increased in 2013. The rate of vegetation change in 2008 compared to 2002 and also in 2013 compared to 2002 were shown in Figs. 7 and 8, respectively.

3.4 The error matrix

In this study, results with high accuracy compared to similar research have been obtained [11]. The reason was the high level of educational points and the accuracy in selecting educational points (polygons). This result is consistent with the theory of Nateghi et al., which considers the acceptable accuracy of land use classification using satellite images to be 85%.

In Table 3, the values of the kappa coefficient and overall accuracy of plant indices calculated for the three years studied are given with the highest NDVI coefficient. The results showed that the kappa index had the best performance in both years and the SAVI index was in the next stage.

In the next step, the indices of product accuracy, user accu-

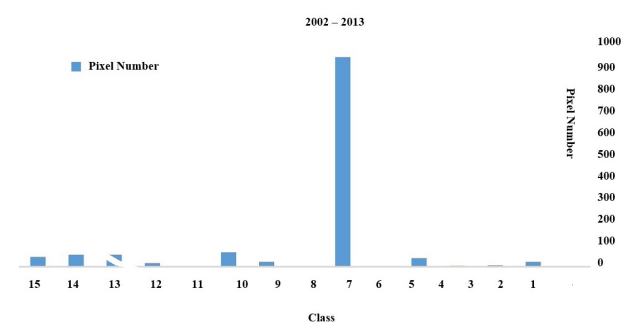


Figure 11. The amount of vegetation changes from 2002 to 2013 in each of the codes.

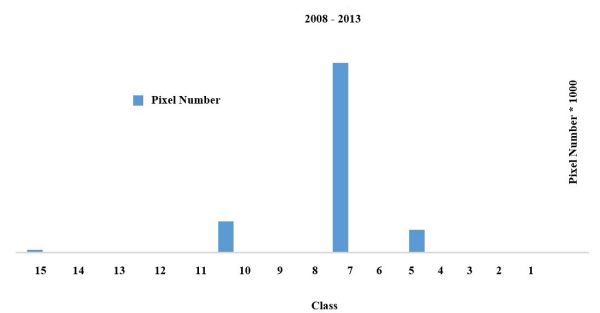


Figure 12. The amount of vegetation changes from 2008 to 2013 in each of the codes.

racy, total accuracy, and kappa coefficient were calculated and the accuracy of the final map was tested according to the error matrix tables (Table 4). Kappa coefficient and overall accuracy deal only with the whole classification and do not provide information about individual classes or the spatial distribution of the error. Other parameters such as user accuracy and product accuracy are used to estimate the accuracy of the classes separately, as shown in Table 4. In this study, the results of the NDVI index with higher accuracy compared to the other index estimated in this study (SAVI) have been obtained. Analyzing Table 4, it can be concluded that the highest product accuracy is related to lands with medium vegetation for all studied indicators and the lowest product accuracy is related to areas without vegetation for all indicators in all three periods. Among the studied indices, NDVI index coefficients were higher. According to the obtained results, the NDVI index with the highest kappa coefficient of 0.84 in 2013 and 0.83 in 2008 and also 0.81 in 2002 had a better performance than other indices. The findings from this study indicate that high-resolution RS imagery can extract and classify vegetation with a satisfactory result.

Table 5 indicates that the vegetation has changed in each period compared with the previous period. So that the area of good vegetation cover was 19,278 ha in 2002, which increased to 22,971 ha in 2008 and decreased to 20,499 ha in 2013. The medium vegetation class comprised 104,985 ha of the land in 2002, which increased to 136,128 ha in 2008 and decreased to 108,340 ha in 2013. The very poor class comprised 283786 ha in 2002, which decreased to 253346 ha in 2008 and increased to 284308 ha in 2013.

Figures 8 and 9 presents the rate of vegetation change in 2008 compared to 2002 and change in 2013 compared to 2002, respectively. Also, Figures 10, 11 and 12 shows the amount of vegetation changes from 2002 to 2008, 2002 to 2013 and 2008 to 2013 in each of the codes respectively. According to Fig. 12 the largest change occurred in the Class 7 code with a total of 8,040,662 pixels. In other words, very poor vegetation changed into moderate vegetation in 2008. After this class, changes in code 10 (average vegetation to very poor vegetation) and code 5 (very poor vegetation to the no vegetation class) are in second and third places, respectively.

4. Conclusion

The purpose of this study was to monitor the changes of vegetation area and diversity in Sirjan Salt lake Using Remote Sensing Data based on the comparison method after classification in the land use map of each sensor. It is of importance to obtain information about vegetation statuses such as their levels and distribution. The use of RS systems is currently an indispensable component of environmental studies [28]. Different VIs are used to identify and detect vegetation, each of which has advantages and disadvantages depending on the study area. In this study, the NDVI was used to identify and extract vegetation in the SSP, and a vegetation map was prepared for each period to compare the vegetation areas in different periods. The study of the SSP from satellite images shows that this area is composed of different parts: the main part of the salt marsh, in which relatively little water is collected during the rainy season, and the lake marginal parts, which appear as dried salt marshes.

After extracting the vegetation using the NDVI, considering the means and standard deviations in the satellite images of each period, the vegetation of the study area was divided into four classes of good, average, very poor, and no vegetation. The results showed that the area of good vegetation cover was 19,278 ha in 2002, which increased to 22,971 ha in 2008 and decreased to 20,499 ha in 2013. The medium vegetation class comprised 104,985 ha of the land in 2002, which increased to 136,128 ha in 2008 and decreased to 108,340 ha in 2013. The very poor class comprised 283786 ha in 2002, which decreased to 253346 ha in 2008 and increased to 284308 ha in 2013. There is very low-density vegetation around SSP and mainly includes halophytes. Since the vegetation of the region is composed of xerophyte species, fluctuations in rainfall have not affected the vegetation, which has also been confirmed during local studies. Accordingly, it can be deduced that the vegetation diversity has not changed in this area.

It is difficult to study vegetation by RS in areas where vegetation canopy is less than 40% due to the reflection of soil and rocks, but the vegetation status of these areas can be detected with the use of VIs and appropriate methods. Jabbari et al. concluded that the substrate soil covered vegetation reflection in poor vegetation, and prevented the reflection of vegetation in the image, resulting in reduced NDVI or similar NDVI values in different areas [29]. Ming Lee and Chung Yeh considered the NDVI index as the most general index in assessing vegetation and many researchers have used this index in their studies [30]. The results of the kappa coefficient of production maps based on vegetation indices and comparison of images of vegetation indices in each sensor with its land-use map indicate that the NDVI vegetation index was better than the SAVI index. Because in this index, the slope of the soil line is used and the negative effects of the underlying soil are well removed and the vegetation separation is done more accurately and the results of this section are in line with the results [31, 32]. According to the obtained results, the NDVI index with the highest kappa coefficient of 0.84 in 2013 and 0.83 in 2008 and also 0.81 in 2002 had a better performance than the

SAVI index. This result indicates the ability of vegetation to distinguish from other land features and better performance of this indicator in detecting changes, which is consistent with the results of Allbed et al. [32]. This is consistent with the results of research by Darwish and Faour, and Ming Lee and Chung Yeh who rated the NDVI vegetation index as the best indicator for vegetation assessment [30, 33].

The relatively low correlation coefficients indicate that in arid regions with low vegetation percentage, the predominance of the substrate soil on the one hand and the nonlinear nature of the correlation relationships between spectral reflectance and vegetation characteristics, on the other hand, result in lower correlation coefficients. Masoud and Koike pointed out the ability of the SAVI index to highlight the scattered vegetation of desert areas [34]. Huete introduced the SAVI index as a hybrid index of relative and distance indices [35]. The results indicate that the ASTER sensor images have the necessary ability for preparing a vegetation map in the SSP, which can confidently be generalized to desert areas. It should be noted that the final accuracy of production maps for such studies depends on the accuracy of field measurements, both concerning the use of sampling methods and in terms of determining suitable and correct sampling sites. Additionally, the accuracy of received data and the methods of image processing and data analysis can play an important role in improving the accuracy of studies. The result of the vegetation study shows that the SSP has directly affected the density of plant species. Bare, vegetation-free lands are visible immediately around the playa due to the soil salinity and the high groundwater that makes salt available to plants, and denser vegetation is observed with increasing distance from the salt playa due to the presence of soils and proper drainage [36]. These results are consistent with those of Quevedo and Frances and Jafari et al. who showed that soil salinity and texture were important factors in the establishment of vegetation in these areas [6, 37].

Overall, modeling of vegetation index and main bands shows that a decrease in vegetation percentage increases the effects of substrate soil and reduces the sensitivity of single bands to vegetation so that the substrate soil affects and overcomes the effect of plant reflection. Therefore, the reflection from a surface with vegetation coverage will be a combined reflection of vegetation and substrate soil, and separation of these two from each other makes the conditions for using satellite single-band information more difficult and the RS technique fails to estimate vegetation characteristics using single-band data. The results showed that individual VIs for each image has specific disadvantages and advantages in different situations. Therefore, the type of sensor, characteristics, and conditions of the study area, knowledge of the type and level of vegetation, and the type of land uses should be considered in the selection of the most appropriate method. For these areas, simultaneous application of several indices also provides better results in the detection and separation of the vegetation level. However, the most appropriate method should be selected with a high accuracy depending on the regional characteristics based on the

highest correlation to use the most efficient indices and analyses and provide appropriate models to monitor and study the vegetation of the study area and areas with similar features.

Due to the special climatic conditions, monitoring and study of vegetation in arid and semi-arid regions are of special importance for applying correct soil and land management methods. Therefore, using LANDSAT satellite images, we can understand the development or destruction process in these areas, especially the vegetation of the area. In this case, the use of LANDSAT satellite imagery provides accurate information with less cost and time at regional and regional scales to implement optimal management methods and achieve the desired results. Finally, additional studies on these areas can help to identify the reasons for the increase and decrease in the areas under study and be useful in developing management strategies in the area.

Acknowledgements:

The authors would like to thank Kerman Environment Organization to provide the secondary data and help us with data preprocessing.

Conflict of interest statement:

The authors declare that they have no conflict of interest.

References

- [1] A. Ghobadian. *Pedology of arid and semi-arid regions*. Amidi Publications, 1th edition, 1984.
- [2] A. Karam, T. Kiani, A. Dadrasi Sabzevar, and Z. Davarzani. "Estimating soil salinity by using remote sensing data and spatial statistics in Sabzevar region". *Quantitative Geomorphological Research*, **7**:31–53, 2019.
- [3] A. U. Gomrokchi, M. Akbari, A. Hassanoghli, and M. Younesi. "Monitoring soil salinity and vegetation using multispectral remote sensing data in interceptor drain of salt marsh in Qazvin Plain". *Geography and Environmental Sustainability*, **10**:37–52, 2020.
- [4] A. H. Mardi, A. Khaghani, A. B. MacDonald, P. Nguyen, N. Karimi, and P. Heidary. "The Lake Urmia environmental disaster in Iran: A look at aerosol pollution". *Science of the Total Environment*, **633**:42–49, 2018.
- [5] A. Sharifian Bahraman, A. Sepehry, and H. Barani. "Plant responses to individual and combined effects of abiotic stress: *Lycium depressum* L. vegetative parameters under salinity and drought". *Journal of Rangeland Science*, **10**:228–243, 2020.
- [6] M. Jafari, M. A. Zareh Chahouki, A. Tavili, and H. Azarnivand. "Effective environmental factors in the distribution of vegetation types in Poshtkouh rangelands of Yazd Province". *Iran. J. Arid Environ.*, **56**:627–641, 2004.
- [7] M. Mumipour. "Temporal and spatial variation of soil salinity variations in a 24-year Period in Abadan District using satellite images". *Geography and Environmental Sustainability*, **8**:47–58, 2018.
- [8] A. Ahmadi, M. Gomarian, and M. Sanjari. "Variations in forage quality of two halophyte species, *Camphorosma monspeliaca* and *Limonium iranicum* at three phenological stages". *Journal of Rangeland Science*, **3**:245–255, 2013.
- [9] W. Ennajia, A. Barakata, I. Karaouib, M. E. Baghdadia, and A. Ariouab. "Remote sensing approach to assess salt-affected soils in the northeast part of Tadla plain, Morocco". *Geology, Ecology, and Landscapes*, **2**:22–28, 2018.
- [10] M. A. Khan and D. J. Weber. *Ecophysiology of high salinity tolerant plants*, volume **9**. Springer, 1th edition, 2006.
- [11] S. Nateghi, A. Nohegar, A. H. Ehsani, and O. Bazrafshan. "Evaluation of vegetation changes based upon vegetation indices using remote sensing". *Iranian Journal of Range and Desert Research*, **24**:778–790, 2018.
- [12] M. Pour Khosravani, A. A. Vali, T. Mahmudi Mohammad Abadi, and N. Salari. "Analysis of ripple mark forms and Nebka obstacles in Sirjan playa". *National Geographic Resolution*, **45**:77–94, 2013.
- [13] M. Yamani and A. Mazidi. "Investigation of changes in the surface and vegetation of Siahkuh desert using remote sensing data". *Geographical Research*, **64**:1–12, 2007.
- [14] M. Ahmadi Nadoushan, A. Soffianian, and S. J. Khajeddin. "Exploring land cover changes of Arak using GIS and Remote Sensing". *Journal of Environmental Science and Technology*, **16**:381–393, 2014.
- [15] D. Yarahmadi. "Autological hydroclimate analysis of Urmia Lake water fluctuations". *National Geographic Resolution*, **46**:92–77, 2014.
- [16] R. Kardan, Q. Azizi, R. Zavar, and H. Muhammadi. "Modeling the impact of the lake on adjacent areas (Case study: Climatic modeling of Jazmourian watershed with the creation of an artificial lake)". *Iran. Watershed Manage. Sci. Eng.*, **3**:15–22, 2009.
- [17] X. Zhou, O. Ooka, H. Chen, Y. Kawamoto, and H. Kikumoto. "Impacts of inland water area changes on the local climate of Wuhan, China". *Indoor and Built Environment*, **25**:296–313, 2016.
- [18] C. Sun, Y. Liu, S. Zhao, M. Zhou, Y. Yang, and F. Li. "Classification mapping and species identification of salt marshes based on a short-time-interval NDVI time-series from HJ-1 optical imagery". *International Journal of Applied Earth Observation and Geoinformation*, **45**:27–41, 2016.

- [19] C. Sun, Y. Liu, and S. Fagherazzi. “Classification mapping of salt marsh vegetation by flexible monthly NDVI time-series using Landsat imagery”. *Estuarine, Coastal and Shelf Science*, **213**:61–80, 2018.
- [20] E. Westinga, A. P. R. Beltran, C. A. J. M. de Bie, and H. A. M. J. van Gils. “A novel approach to optimize the hierarchical vegetation mapping from hyper-temporal NDVI imagery demonstrated at national level for Namibia”. *International Journal of Applied Earth Observation and Geoinformation*, **91**:102152, 2020.
- [21] R. H. Maneja, J. D. Miller, W. Li, H. El-Askary, A. V. B. Flandez, and J. J. Dagoy. “Long-term NDVI and recent vegetation cover profiles of major offshore island nesting sites of sea turtles in Saudi waters of the northern persian Gulf”. *Ecological Indicators*, **117**:106612, 2020.
- [22] K. P. Woodbridge, S. Pirasteh, and D. R. Parsons. “Investigating fold-river interactions for major rivers using a scheme of remotely sensed characteristics of river and fold geomorphology”. *Remote Sensing*, **11**:2037, 2019.
- [23] J. W. Rouse, R. H. Haas, J. A. Schell, and D. W. Deering. *Monitoring vegetation systems in the Great Plains with ERTS*. NASA Special Publications, 1th edition, 1974.
- [24] P. S. Chavez. “Image-based atmospheric corrections: Revisited and improved”. *Photogrammetric Engineering and Remote Sensing*, **62**:1025–1036, 1996.
- [25] H. Safdar, A. Amin, Y. Shafiq, A. Ali, R. Yasin, and M. I. Sarwar. “A review: Impact of salinity on plant growth”. *Natural Sciences*, **17**:34–40, 2019.
- [26] L. Bharathkumar and M. A. Mohammed Aslam. “Crop pattern mapping of tumkur taluk using NDVI technique: a remote sensing and GIS approach”. *Aquatic Procedia*, **4**:1397–1404, 2015.
- [27] A. Karimi, S. Abdollahi, H. R. Kabiri Balajadeh, K. Ostad-Ali-Askari, S. Eslamian, and V. P. Singh. “The use of remote sensing techniques in detecting and predicting forest vegetation change using MODIS satellite data, Golestan, Iran”. *American Journal of Engineering and Applied Sciences*, **11**:387–396, 2018.
- [28] L. Guerine, M. Belgourari, and H. Guerinik. “Cartography and diachronic study of the Naama sabkha (Southwestern Algeria) remotely sensed vegetation index and soil properties”. *Journal of Rangeland Science*, **10**:172–187, 2020.
- [29] S. Jabbari, S. J. Khajedin, R. Jafari, and S. Soltani. “Investigation of changes in range vegetation percentage using satellite images in Semirom area of Isfahan”. *Journal of Applied Ecology*, **3**:27–38, 2014.
- [30] T. M. Lee and H. C. Yeh. “Applying remote sensing techniques to monitor shifting wetland vegetation: A case study of Danshui River estuary mangrove communities, Taiwan”. *Ecological Engineering*, **35**:487–496, 2009.
- [31] J. G. P. W. Clevers. “Beyond NDVI: extraction of biophysical variables from remote sensing imagery”. *Land Use and Land Cover Mapping in Europe*, **18**:363–381, 2014.
- [32] A. Allbed, L. Kumar, and Y. Aldakheel. “Assessing soil salinity using soil salinity and vegetation indices derived from IKONOS highspatial resolution imageries: Applications in a date palm dominated region”. *Geoderma*, , 2014.
- [33] T. Darwish and G. Faour. “Rangeland degradation in two watersheds of Lebanon”. *Lebanese Science Journal*, **9**:71–80, 2008.
- [34] A. A. Masoud and K. Koike. “Arid land sanitization detected by remotely sensed land cover changes: A case study in the Siwa region, NW Egypt”. *Journal of Arid Environments*, **66**:151–167, 2006.
- [35] A. R. Huete. “A soil-adjusted vegetation index (SAVI)”. *Remote Sensing of Environment*, **25**:295–309, 1988.
- [36] A. Ahmadi, A. Kazemi, and H. Toranjzar. “Comparison of spectrum indices for mapping soil salinity in saline lands of Chezan plain (Markazi province)”. *Desert*, **23**:211–220, 2018.
- [37] D. I. Quevedo and F. Frances. “A conceptual dynamic vegetation–soil model for arid and semiarid zones”. *Hydrology and Earth System Sciences*, **12**:1175–1187, 2008.